A Systematic Bit-Wise Decomposition of M-ary Symbol Metric

Chia-Wei Chang, *Member, IEEE*, Po-Ning Chen, *Senior Member, IEEE,* and Yunghsiang S. Han, *Member, IEEE*

***Abstract*— In this paper, we present a systematic recursive formula for bit-wise decomposition of M-ary symbol metric. The decomposed bit metrics can be applied to improve the performance of a system where the information sequence is binary-coded and interleaved before M-ary modulated. A traditional receiver designed for certain system is to de-map the received M-ary symbol into its binary isomorphism so as to facilitate the subsequent bit-based manipulation, such as hard-decision decoding. With a bit-wise decomposition of M-ary symbol metric, a soft-decision decoder can be used to achieve a better system performance.**

The idea behind the systematic formula is to decompose the symbol-based maximum-likelihood (ML) metric by equating a number of specific equations that are drawn from squared-error criterion. It interestingly yields a systematic recursive formula that can be applied to some previous work derived from different standpoint. Simulation results based on IEEE 802.11a/g standard show that at bit-error-rate of 10^{-5}, the proposed bit-wise decomposed metric can provide 3.0 dB, 3.9 dB and 5.1 dB improvement over the concatenation of binary-demapper, deinterleaver and hard-decision decoder respectively for 16QAM, 64QAM and 256QAM symbols, in which the in-phase and quadrature components in a complex M^2-QAM symbol are independently treated as two real M-PAM symbols. Further empirical study on system imperfection implies that the proposed bit-wise decomposed metric also improves the system robustness against gain mismatch and phase imperfection. In the end, a realization structure that avails the recursive nature of the proposed bit-decomposed metric formula is addressed.

***Index Terms*— Maximum-likelihood decoding, QAM modulation, soft-decision decoding, Viterbi decoder.**

I. INTRODUCTION

THE state-of-the-art wireless transmission technique of IEEE 802.11a/g [8], [9] incorporated high QAM into OFDM to achieve a high data rate. In order to make a better use of the error correcting capability of the adopted (2,1,6) convolutional code, the standard specified a two-step bit interleaver, where the first step maps adjacent code bits onto non-adjacent sub-carriers, and the second step permutes the code bits alternately onto less and more significant bits of the QAM constellation. Such an interleaver design, although straight and simple in concept, may restrict the potential structures of a receiver in practice.

For a system where the binary information sequence is encoded and bit-interleaved before M-ary modulated, a traditional receiver design is to de-map the received M-ary symbol into its binary isomorphism so as to facilitate the subsequent bit-based manipulation as shown in Fig. 1. Take IEEE std. 802.11a as an example. After de-interleaving, the two code bits, c_1 and c_2, that decide a trellis branch of (2,1,6) convolutional code will respectively come from the least significant bit of 16QAM quadrature component r_1 and the most significant bit of 16QAM quadrature component r_7 [8]. The dependence of one single trellis branch on two time-inconsecutive QAM quadrature symbols somehow suggests that the received M-ary symbol should be hard-demapped before decoding, since other receiver structure such as one with soft-decision decoding may require a branch metric that can be determined by two distant and non-orderly M-ary symbols. Such a soft-decision-based receiver will become more involved, when a receiver structure that also supports multi-rate transmission through code punctuation is further considered.

In order to design a general receiver for use of M-ary symbol transmission of coded and interleaved information sequence, researchers have proposed several heuristic methods to perform bit-wise decomposition of M-ary symbol metric [10], [12], [15]. With a bit-wise decomposition of M-ary symbol metric, a better system performance can possibly be achieved by adopting a soft-decision decoder, even if code punctuation for dynamic rate transmission is incorporated. Even though some of them perform well in practice, there is still lack of a systematic method for bit-wise decomposition of M-ary symbol metric. Thus, we propose in this work a general recursive formula for bit-wise decomposition of M-ary symbol metric[4]. The proposed approach is to approximate the symbol-based maximum-likelihood (ML) metric by equating a number of specific equations that are drawn from square error criterion. Notably, the square error between symbol-based ML metric and its bit-decomposed approximation reduces to zero when all the listed equations can be simultaneously satisfied, which means that the performance of the symbol-based ML metric can be achieved by taking the proposed bit-wise decomposed metrics. This optimistic result of zero square error however can not be obtained in general due to the bit-wise interleaving.

Manuscript received May 14, 2004; revised June 6, 2005 and April 17, 2006; accepted July 17, 2006. The editor coordinating the review of this paper and approving it for publication is L. Vandendorpe. This work was supported by the National Science Council, Taiwan, R.O.C., under Grant NSC 92-2213-E- 009-118, 93-2213-E-009-050 and 94-2213-E-009-017.

C.-W. Chang is with the Dept. of ECE, University of California, San Diego, CA 92093 USA (e-mail: sekwan.cm87@nctu.edu.tw).

P.-N. Chen is with the Dept. of Communications Eng., National Chiao Tung Univ., Taiwan, R.O.C. (e-mail:qponing@mail.nctu.edu.tw).

Y. S. Han was with the Dept. of CSIE, National Chi Nan University, Taiwan. Now he is with the Graduate Institute of Communication Engineering, National Taipei University, Taiwan, R.O.C. (e-mail: yshan@mail.ntpu.edu.tw).

Digital Object Identifier 10.1109/TWC.2006.04322

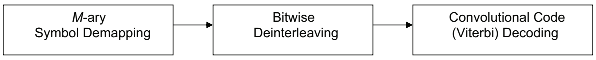

Fig. 1. An exemplified receiver design.

A suboptimal bit-decomposition metric in terms of maximal subset of simultaneously satisfiable equations is then proposed. Exemplified study on QAM modulation interestingly yields a systematic recursive bit metric formula. By re-examining their metrics, we interestingly found that the bit reliability metrics of some previous work also have similar recursive forms. Details are given in Section II-C.

Empirical study under the system setting of IEEE 802.11a/g and the additive white Gaussian noise (AWGN) channel showed that at bit error rate (BER) = 10^{-5}, the proposed bit-decomposed metric has 3.0 dB, 3.9 dB and 5.1 dB gains over the hard decision system for 16QAM, 64QAM and 256QAM, respectively. Also, only 0.13 dB performance degradation is resulted by introducing 32-level quantization for 16QAM signals. The quantization impact for 64QAM signals under 64-level uniform quantization can even be reduced to 0.07 dB. No further performance degradation, in addition to that due to quantization, can be observed, when mismatch of AGC gain is limited to be within $\pm 40\%$. The robustness of the proposed bit-decomposed metric against phase imperfection is also examined. When the phase drift increases up to $\pm 6^o$, the BER due to our bit-decomposed metric will increase from 10^{-5} to around 4×10^{-5} at $E_b/N_0 = 6.7$ dB for 16QAM modulation. This phase drift tolerance reduces to $\pm 4^o$ at $E_b/N_0 = 9.7$ dB for 64QAM modulation, where E_b/N_0 is chosen such that the no-phase-drift BER is approximately 10^{-5}.

Some previous works on bit reliability study are summarized below. In [15], Zehavi proposed a decoding scheme that consists of a sub-optimal Log-Likelihood-Ratio (LLR) bit demapping for subsequent use of path metric computation of Viterbi decoder. Later, Pyndiah et al. [10] provided a pragmatic algorithm based on LLR to turbo codes associated with high QAM modulation, and showed that the block turbo-coded QAM modulation outperforms Trellis-Coded Modulation (TCM) scheme by at least 1 dB at BER = 10^{-5}. Then, Caire et al. [3] presented a maximum-likelihood bit demapping for bit-interleaved coded modulation (BICM) and gave guidelines for its design. Tosato and Bisaglia [12] adapted the Pyndiah's algorithm to COFDM system, and proposed a simplified bit reliability decomposition for 16QAM and 64QAM constellations. Their simulations showed that for 64QAM constellation, adopting their bit reliability decomposition results in 8.5 dB gain at BER = 10^{-4} over a hard-decision-based receiver under HIPERLAN/2 system model.[1]

This paper is organized in the following fashion. Section II provides the analysis of the proposed bit-decomposed metric, followed by its complexity comparison with other soft-demapping schemes. Section III summarizes the simulation results over AWGN channels, and examines the robustness of the proposed bit-decomposed metric against system imperfection. Section IV provides a realization structure for our proposed bit-wise decomposition of M-ary symbol metric. Concluding remarks appear in Section V.

[1]Similar to IEEE std 802.11a/g, the scrambled input sequence of HIPERLAN/2 [5] is convolutionally encoded with rate $1/2$ and constraint length 7 before bit-wise interleaving and QAM modulation.

II. SYSTEMATIC BIT-WISE DECOMPOSITION OF M-ARY SYMBOL METRIC

Denote by $\boldsymbol{r} = (r_1, r_2, \ldots, r_K)$ the real-valued received vector when M-ary symbols $\boldsymbol{s} = (s_1,\, s_2,\, \ldots,\, s_K)$ that are mapped from an interleaved version of encoding output $\boldsymbol{c} = (c_1, c_2, \ldots, c_N) \in \{0,1\}^N$ are transmitted. Assume that the M-ary symbol transmission suffers additive white Gaussian noise (AWGN), $n_1, n_2, n_3, \ldots, n_K$, with single-sided noise power per hertz N_0. The received vector $\boldsymbol{r}$ then satisfies

$$r_i = s_i + n_i$$

for $1 \le i \le K$. For the AWGN channel, the maximum-likelihood decision upon the receipt of $\boldsymbol{r}$ is given by:

$$\begin{aligned} d_{ML}(\boldsymbol{r}) &= \arg\max_{\boldsymbol{s}\in\mathcal{S}} \Pr\{r_1, \ldots, r_K \,|s_1, \ldots, s_K\} \\ &= \arg\max_{\boldsymbol{s}\in\mathcal{S}} \frac{1}{(\pi N_0)^{K/2}} \exp\left\{-\sum_{i=0}^{K} \frac{(r_i - s_i)^2}{N_0}\right\} \\ &= \arg\min_{\boldsymbol{s}\in\mathcal{S}} \sum_{i=1}^{K} (r_i - s_i)^2, \end{aligned} \tag{1}$$

where $\mathcal{S}$ represents the set of all possible mappings from the convolutional codeword in $\mathcal{C}$ to its respective symbol word. Due to the non-linear (e.g., interleaving) relation between codeword $\boldsymbol{c}$ and transmitted symbol $\boldsymbol{s}$, Eq. (1) cannot be equivalently transformed to the sum of code bit metrics. An approximation is therefore necessary to perform soft-decision decoding. Our goal then becomes to find a sequence of function $\boldsymbol{\eta} = (\eta_1, \eta_2, \ldots, \eta_N)$ such that the sum of all code symbol metrics, $\sum_{i=1}^{K}(r_i - s_i)^2$, can be well-approximated by $\sum_{i=1}^{N} \eta_i(c_i, \boldsymbol{r})$ for every mapping pair ($\boldsymbol{c}$, $\boldsymbol{s}$) and the received vector $\boldsymbol{r}$, where functions $\eta_1, \eta_2, \ldots, \eta_N$ can be distinct bit-metric functions.

For clarity and simplicity, we use the 16QAM modulation as an example for the presentation of our subsequent derivation in this section. The general results for 64QAM and 256QAM will be given at the end. Let $s(\cdot,\cdot)$ be the real quadrature 4PAM mapping from the code bit to the transmitted symbol, and denote by $\sigma(\cdot)$ the bit-interleaving function mapping. Then, received vector component r_i is given by the sum of transmitted symbol $s(c_{\sigma(2i-1)}, c_{\sigma(2i)})$ and noise n_i. Here, the in-phase and quadrature components are independently treated as received scalars due to the transmission of real 4PAM symbols although our system presumes complex 16QAM constellation.

As r_i is only a function of code bits $c_{\sigma(2i-1)}$ and $c_{\sigma(2i)}$, its contribution to the summation in (1) is equal to $[r_i - s(c_{\sigma(2i-1)}, c_{\sigma(2i)})]^2$. Because $r_1, \ldots, r_{i-1}, r_{i+1}, \cdots, r_K$ are nothing to do with $c_{\sigma(2i-1)}$ and $c_{\sigma(2i)}$, we can simplify our goal to the finding of functions η_{2i-1} and η_{2i} such that $\eta_{2i-1}(c_{\sigma(2i-1)}, r_i) + \eta_{2i}(c_{\sigma(2i)}, r_i)$ well-approximates $[r_i - s(c_{\sigma(2i-1)}, c_{\sigma(2i)})]^2$ for all legal $c_{\sigma(2i-1)}$ and $c_{\sigma(2i)}$ in the codebook. Since function pairs (η_{2i-1}, η_{2i}) are determined according to independent and identical statistical structure, it is reasonable to presume that they are universal for all received scalars, and hence, we can set , $\eta_{2i-1} = f_1$ and $\eta_{2i} = f_2$ for some functions f_1 and f_2 for $1 \le i \le K$.[2]

We next address the criterion of "well-approximation" adopted in this paper.

A. Equating the Coefficients in Squared Error

The criterion we adopt is the minimization of average square error, namely,

$$\min_{f_1, f_2} E\left[\left(f_1(c,r) + f_2(\bar{c},r) - [r - s(c,\bar{c})]^2\right)^2\right], \tag{2}$$

where the expectation is taken over the statistics of c, $\bar{c}$ and r. Without loss of generality, we can re-write f_1 and f_2 as:[3]

$$f_1(c,r) = \frac{1}{2}r^2 + a_{1,c,r}r + b_{1,c,r} \quad f_2(\bar{c},r) = \frac{1}{2}r^2 + a_{2,\bar{c},r}r + b_{2,\bar{c},r}.$$

This transforms (2) into minimization of

$$E\left[\left[(a_{1,c,r} + a_{2,\bar{c},r} + 2s(c,\bar{c}))\, r + \left(b_{1,c,r} + b_{2,\bar{c},r} - s^2(c,\bar{c})\right)\right]^2\right] \tag{3}$$

subjected to $a_{1,c,r}$, $a_{2,\bar{c},r}$, $b_{1,c,r}$, $b_{2,\bar{c},r}$.

It is neither practical nor analytically tractable to consider general coefficient functions, $a_{1,c,r}$, $a_{2,\bar{c},r}$, $b_{1,c,r}$ and $b_{2,\bar{c},r}$, for continuous r. Instead, we consider a piece-wise simplification of them by setting $a_{1,c,r}$, $a_{2,\bar{c},r}$, $b_{1,c,r}$ and $b_{2,\bar{c},r}$ equal to a constant for $r \in \mathcal{I}_\rho = (\lambda_{\rho-1}, \lambda_\rho]$, where $1 \le \rho \le q$ and $-\infty = \lambda_0 \le \lambda_1 \le \cdots \le \lambda_q = \infty$. Apparently, there will be totally $4q$ constants and $(q-1)$ interval thresholds to be determined. For notational convenience, we use $a_{1,c,\rho}$, $a_{2,\bar{c},\rho}$, $b_{1,c,\rho}$ and $b_{2,\bar{c},\rho}$ to denote the constant values specified for each interval. This reduces (3) to the minimization of

$$\sum_{\rho=1}^{q} \Pr\{r \in \mathcal{I}_\rho\}\, E\left[\left[(a_{1,c,\rho} + a_{2,\bar{c},\rho} + 2s(c,\bar{c}))\, r + \left(b_{1,c,\rho} + b_{2,\bar{c},\rho} - s^2(c,\bar{c})\right)\right]^2 \middle| r \in \mathcal{I}_\rho\right]. \tag{4}$$

Intuitively from (4) , if all coefficients of r, namely, $a_{1,c,\rho} + a_{2,\bar{c},\rho} + 2s(c,\bar{c})$ and $b_{1,c,\rho} + b_{2,\bar{c},\rho} - s^2(c,\bar{c})$, can be made zero by some specific $\{(a_{1,c,\rho}, a_{2,\bar{c},\rho})\}_{\rho=1}^q$ and $\{(b_{1,c,\rho}, b_{2,\bar{c},\rho})\}_{\rho=1}^q$ for some finite q, Eq. (4) will be exactly zero. As a result, we list the coefficients in (4) according to the value of $s(c,\bar{c})$, and let them be zero.

$$\begin{aligned}
&a_{1,0,\rho} + a_{2,0,\rho} + 2\cdot s(0,0) = 0, \ \ b_{1,0,\rho} + b_{2,0,\rho} - s^2(0,0) = 0\\
&a_{1,0,\rho} + a_{2,1,\rho} + 2\cdot s(0,1) = 0, \ \ b_{1,0,\rho} + b_{2,1,\rho} - s^2(0,1) = 0\\
&a_{1,1,\rho} + a_{2,1,\rho} + 2\cdot s(1,1) = 0, \ \ b_{1,1,\rho} + b_{2,1,\rho} - s^2(1,1) = 0\\
&a_{1,1,\rho} + a_{2,0,\rho} + 2\cdot s(1,0) = 0, \ \ b_{1,1,\rho} + b_{2,0,\rho} - s^2(1,0) = 0
\end{aligned}$$

It can be seen that the solution should be a function of the mapping $s(\cdot,\cdot)$ adopted.

[2]As a consequence, the number of distinct functions among $\eta_1, \eta_2, \ldots, \eta_N$ is $m = \log_2(M)$ for real M-PAM modulation, which will be denoted by $f_1, f_2, \ldots, f_m$ in the sequel. These bit metric functions, $f_1, f_2, \ldots, f_m$, will be applied to decompose the symbol metric for every QAM quadrature component symbol received.

[3]The optimal $f_1^*(c,r)$ can apparently be re-expressed as $(1/2)r^2 + (f_1^*(c,r)/r - r/2)r + 0$. Therefore, as long as the coefficient $a_{1,c,r} = (f_1^*(c,r)/r - r/2)$ and $b_{1,c,r} = 0$ are allowed to be r-dependent, the form of $(1/2)r^2 + a_{1,c,r}r + b_{1,c,r}$ does cover the optimal solution.

A common mapping used in practice for PAM modulation is the Gray code mapping. For 16QAM quadrature component, we can number the equations according to ascending value of $s(\cdot,\cdot)^4$ and yield:

$$a_{1,0,\rho} + a_{2,0,\rho} - 6 = 0, \quad b_{1,0,\rho} + b_{2,0,\rho} - 9 = 0 \tag{5a}$$
$$a_{1,0,\rho} + a_{2,1,\rho} - 2 = 0, \quad b_{1,0,\rho} + b_{2,1,\rho} - 1 = 0 \tag{5b}$$
$$a_{1,1,\rho} + a_{2,1,\rho} + 2 = 0, \quad b_{1,1,\rho} + b_{2,1,\rho} - 1 = 0 \tag{5c}$$
$$a_{1,1,\rho} + a_{2,0,\rho} + 6 = 0, \quad b_{1,1,\rho} + b_{2,0,\rho} - 9 = 0 \tag{5d}$$

It can be easily verified that at most three of the four equations (5a)–(5d) can be made valid simultaneously. In addition, it is not necessary to equate coefficient equations with non-contiguous equation numbers (e.g., (5a), (5c) and (5d)) because the squared error in (4) can be further reduced by replacing the non-contiguous numbered equation (e.g., (5a)) with one having contiguous equation number (e.g., (5b)). This suggests that among those cases we tried, the best choice that minimizes (4) for Gray code mapping is to take $q = 2$, for which coefficient constants for $\rho = 1$ corresponds to the validity of (5a)–(5c), and those for $\rho = 2$ are selected to validate (5b)–(5d). By experimenting over 64QAM and 256QAM with Gray code mappings, we found that the same observation is also applied.

Based on the above finding, we propose a systematic approach to define a bit-decomposition of M-ary symbol metric specifically for Gray code mapping as follows.

Initialization: List and number the coefficient equations in ascending value of Gray code mapping. (Suppose there are L of them, which are numbered with $1, 2, \ldots, L$.)

Step 1. For each $1 \le \rho \le L$, find the largest set A_ρ of equations

- *that contains equation ρ (namely, the equation whose index equals ρ),*
- *that can be simultaneously made valid, and*
- *that are contiguous in their equation numbers.*

Step 2. Delete all duplicate sets among $A_1, A_2, \ldots, A_L$. (Let q be the number of sets remained.)

Step 3. Output the remaining q distinct equation sets.

Step 4. Determine the optimal $\boldsymbol{\lambda} = (\lambda_1, \ldots, \lambda_q)$ that minimizes the average squared error in (4).

Notably, the solution obtained from the above procedure is only suboptimal in the minimization of average squared error over all legitimate $f_1(c,r)$ and $f_2(\bar{c},r)$. However, simulations introduced later show that at BER = 10^{-5}, the piece-wise simplification of $a_{1,c,r}$, $a_{2,\bar{c},r}$, $b_{1,c,r}$ and $b_{2,\bar{c},r}$ is only 0.83 dB

[4]For 16 QAM, $s(0,0) = -3$, $s(0,1) = -1$, $s(1,1) = +1$, $s(1,0) = +3$.

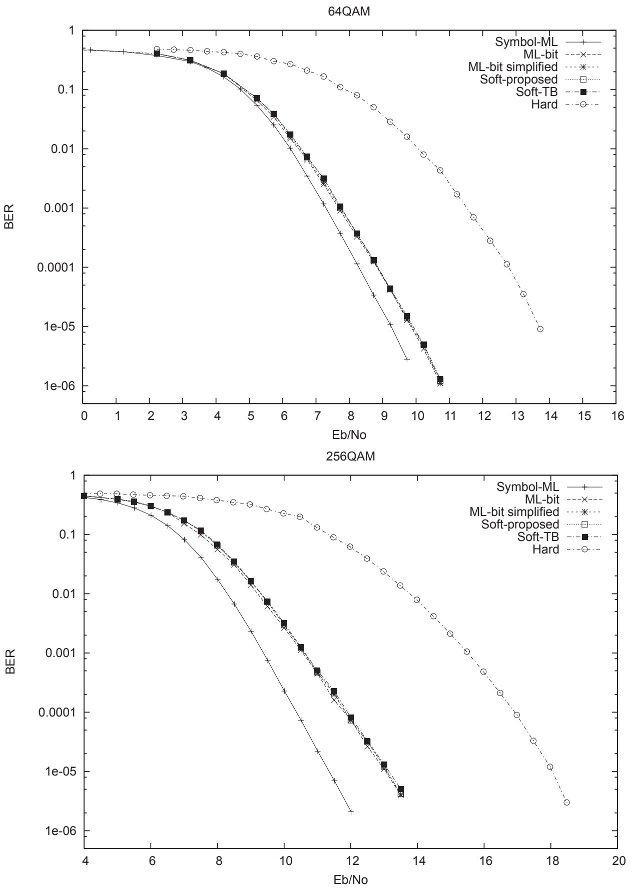

Fig. 2. System performances under AWGN channels.

and 1.4 dB inferior to the *non-achievable*[5] Symbol-ML lower bounds under 64QAM modulation and 256QAM modulation, respectively (cf. Fig. 2). The results indicate that even if the optimal coefficient functions for continuous r are adopted, the performance improvement is very limited. This empirically justifies the use of piece-wise simplifications of the coefficient functions.

B. Bit-Decompositions of 16QAM, 64QAM and 256QAM Symbol Metrics

Applying Step 1 of the proposed algorithm to (5a)–(5d) results:

$$\begin{aligned} A_1 &= \{\text{(5a), (5b), (5c)}\} \\ A_2 &= \{\text{(5a), (5b), (5c)}\} \\ A_3 &= \{\text{(5b), (5c), (5d)}\} \\ A_4 &= \{\text{(5b), (5c), (5d)}\}. \end{aligned}$$

[5] As mentioned earlier, with a nonlinear mapping between codeword $\boldsymbol{c}$ and symbol word $\boldsymbol{s}$, a receiver can no longer implement Eq. (1). However, by turning off the interleaver, which in turn linearizes the relation between $\boldsymbol{c}$ and $\boldsymbol{s}$, a M-ary modulated (2,1,6) convolutional codeword can be decoded by tracing over the code trellis in which each branch metric is determined by exactly one received symbol. Notably, the performance of the symbol-based ML decision with disabled interleaver is an apparent performance lower bound to any bit-demapped schemes under AWGN channels. Thus, by means of the symbol-ML performance curve, one can tell that the improvement margin for a bit-demapped scheme is limited, if it already performs close to the symbol-based ML decision. As a disabled interleaver is not a valid system option for IEEE 802.11a/g system, we therefore term this performance bound *non-achievable*, and only illustrate it for the sake of comparison.

Notably, A_1, A_2, A_3 and A_4 must respectively contain equation (5a), (5b), (5c) and (5d) according to the algorithm. Since $A_1 = A_2$ and $A_3 = A_4$, Step 2 yields $q = 2$. The coefficients that validate the equations in sets A_1 and A_3 are respectively:

$$A_1(\rho = 1) \quad : \quad \begin{cases} a_{1,0,1} = 2 - a_{2,1,1} \\ a_{1,1,1} = -2 - a_{2,1,1} \\ a_{2,0,1} = 4 + a_{2,1,1} \\ b_{1,0,1} = b_{1,1,1} = 1 - b_{2,1,1} \\ b_{2,0,1} = 8 + b_{2,1,1} \end{cases}$$

$$A_3(\rho = 2) \quad : \quad \begin{cases} a_{1,0,2} = 2 - a_{2,1,2} \\ a_{1,1,2} = -2 - a_{2,1,2} \\ a_{2,0,2} = -4 + a_{2,1,2} \\ b_{1,0,2} = b_{1,1,2} = 1 - b_{2,1,2} \\ b_{2,0,2} = 8 + b_{2,1,2} \end{cases}$$

Accordingly, with uniform distributed c and $\bar{c}$, the average squared error becomes:

$$\begin{aligned} W(\boldsymbol{\lambda}) &= \frac{1}{4\sqrt{\pi N_0}} \left(\int_{\lambda_0}^{\lambda_1} (8r)^2\, e^{-(r-3)^2/N_0} dr + \right. \\ &\quad \left. \int_{\lambda_1}^{\lambda_2} (-8r)^2\, e^{-(r+3)^2/N_0} dr \right) \\ &= \frac{16}{\sqrt{\pi N_0}} \left(\int_{-\infty}^{\lambda_1} r^2 e^{-(r-3)^2/N_0} dr + \right. \\ &\quad \left. \int_{\lambda_1}^{\infty} r^2 e^{-(r+3)^2/N_0} dr \right). \end{aligned} \tag{6}$$

Taking the derivative of (6) with respective to λ_1 then concludes that the optimal λ_1 that minimizes $W(\boldsymbol{\lambda})$ is zero, and the average squared error is reduced to

$$8(18 + N_0)\mathrm{erfc}\left(\frac{3}{\sqrt{N_0}}\right) - 48\sqrt{\frac{N_0}{\pi}} \exp\left\{-\frac{9}{N_0}\right\}.$$

We summarize the derivation above as follows.

$$\begin{aligned} f_1(c, r) &= \frac{1}{2}r^2 + a_{1,c,\rho} r + b_{1,c,\rho} \\ &= \frac{1}{2}r^2 + [2(1-2c) - a_{2,1,\rho}]r + (1 - b_{2,1,\rho}) \\ f_2(c, r) &= \frac{1}{2}r^2 + a_{2,c,\rho} r + b_{2,c,\rho} \\ &= \frac{1}{2}r^2 + [a_{2,1,\rho} - 4(1-c)\cdot \mathrm{sgn}(r)]r \\ &\quad + [b_{2,1,\rho} + 8(1-c)], \end{aligned}$$

where

$$\mathrm{sgn}(r) = \begin{cases} 1, & \text{if } r > 0; \\ 0, & \text{if } r = 0; \\ -1, & \text{if } r < 0 \end{cases} \quad \text{and} \quad \rho = \begin{cases} 1, & \text{if } r \le 0; \\ 2, & \text{if } r > 0, \end{cases}$$

and $a_{2,1,1}, a_{2,1,2}, b_{2,1,1}, b_{2,1,2}$ can be any fixed values. Since we can remove the constants in $\sum_{i=1}^{N} \eta_i(c_i, \boldsymbol{r})$ without affecting the decoding result (namely, we can keep only those terms that depend on $\boldsymbol{c}$), and since a universal scaling on all bit-decomposed metric functions also preserves the decoding result, the bit-decomposed metric functions can be equivalently reduced to:

$$\begin{aligned} f_1^{16\text{QAM}}(c, r) &= c|r| \cdot \mathrm{sgn}(-r) \\ f_2^{16\text{QAM}}(c, r) &= c(|r| - 2). \end{aligned}$$

Consequently, we replace $[r_i - s(c_{\sigma(2i-1)}, c_{\sigma(2i)})]^2$ by $f_1^{16\mathrm{QAM}}(r_i, c_{\sigma(2i-1)}) + f_2^{16\mathrm{QAM}}(r_i, c_{\sigma(2i)}) = c_{\sigma(2i-1)}|r_i| \cdot \mathrm{sgn}(-r_i) + c_{\sigma(2i)}(|r_i| - 2)$ for $c_{\sigma(2i-1)}, c_{\sigma(2i-1)} \in \{0, 1\}$ for which a decoding algorithm like Viterbi decoding becomes applicable.

We can similarly obtain the equivalent bit-decomposed metric functions for 64QAM (where the images of quadrature component symbol mapping include -7, -5, -3, -1, 1, 3, 5 and 7) and 256QAM (where the images of quadrature component symbol mapping include -15, -13, …, 13 and 15) under the IEEE 802.11a system setting[6] as:

$$\begin{cases} f_1^{64\mathrm{QAM}}(c,r) &= c(|r-4| + |r| + |r+4| - 8) \cdot \mathrm{sgn}(-r) \\ f_2^{64\mathrm{QAM}}(c,r) &= f_1^{16\mathrm{QAM}}(c, 4-|r|) \\ f_3^{64\mathrm{QAM}}(c,r) &= f_2^{16\mathrm{QAM}}(c, |r|-4) \end{cases}$$

and

$$\begin{cases} f_1^{256\mathrm{QAM}}(c,r) &= c(|r-4| + |r| + |r+4| - 8) \cdot \mathrm{sgn}(-r) \\ & \quad +c(|r-8| + |r+8| - 16) \cdot \mathrm{sgn}(-r) \\ f_2^{256\mathrm{QAM}}(c,r) &= f_1^{64\mathrm{QAM}}(c, 8-|r|) \\ f_3^{256\mathrm{QAM}}(c,r) &= f_2^{64\mathrm{QAM}}(c, |r|-8) \\ f_4^{256\mathrm{QAM}}(c,r) &= f_3^{64\mathrm{QAM}}(c, 8-|r|) \end{cases}$$

We end this subsection by noting that the above result suggests a recursive bit-metric decomposition formula. Specifically, for M-ary PAM modulation (or equivalently, M^2-QAM) with amplitude spacing u,[7]

$$\begin{aligned} f_1^{(m)}(c,r) &= c \cdot \mathrm{sgn}(-r) \sum_{i=-(m-2)}^{m-2} (|r+2ui| - 2ui) \\ f_j^{(m)}(c,r) &= f_{j-1}^{(m-1)}\left(c, (-1)^j\left(2^{m-2}u - |r|\right)\right), \end{aligned}$$

where $m = \log_2(M) \geq 2$, $2 \leq j \leq m$ and $f_1^{(1)}(c,r) = -cr$. Note that m is respectively 2, 3 and 4 for 16QAM, 64QAM and 256QAM. Consequently, after specifying the first-bit metric f_1, the subsequent bit-metrics are alternately the *left-shift mirror* $f_{j-1}^{(m-1)}\left(c, 2^{m-2}u - |r|\right)$ and *right-shift* $f_{j-1}^{(m-1)}\left(c, |r| - 2^{m-2}u\right)$ of the bit-metrics for m less one. Such bit-metric assignment somehow balance the bit reliability for decoding.

C. Bit Metrics Recursively Generated from Other First-Bit Metric

In this subsection, we briefly describe some existing structures of receiver design for M-ary modulated interleaved code.

In 2002, Tosato and Bisaglia [12] has proposed and examined a simplified soft-output demapper for binary interleaved COFDM with application to HIPERLAN/2 [5].[8] We interestingly found that their proposed bit metrics $\{g_j^{(m)}(\cdot,\cdot)\}_{1\leq j\leq m, m\geq 1}$ for 2^{2m}-QAM can be equivalently expressed in terms of our recursive formula as:

$$\begin{aligned} g_1^{(m)}(c,r) &= c(-r) \\ g_j^{(m)}(c,r) &= g_{j-1}^{(m-1)}\big(c, (-1)^j(2^{m-2}u - |r|)\big). \end{aligned}$$

The bit metrics $\{g_j^{(m)}(\cdot,\cdot)\}_{1\leq j\leq m,\ m\geq 1}$ are actually simplified from the bit metrics $\{\bar{g}_j^{(m)}(\cdot,\cdot)\}_{1\leq j\leq m,\ m\geq 1}$ derived from the bit-based log-likelihood ratio (LLR) decision [12], which can also be re-expressed using our recursive formula as:

$$\begin{aligned} \bar{g}_1^{(m)}(c,r) &= \frac{1}{2} \cdot c \cdot \mathrm{sgn}(-r) \sum_{i=0}^{m-1} (|r+ui| + |r-ui| - 2ui) \\ \bar{g}_j^{(m)}(c,r) &= \bar{g}_{j-1}^{(m-1)}\big(c, (-1)^j(2^{m-2}u - |r|)\big). \end{aligned}$$

Note that Tosato and Bisaglia's simplified formulas (or the original LLR formulas) are different from our bit metrics only on the initial functions. This suggests that by varying the first-bit metric, variants of bit-decomposed metrics can be resulted through the recursive formula we established. As anticipated, with $f_1^{(m)} = g_1^{(m)}$ for $m = 1, 2$, our bit decomposed metric coincides with that proposed in [12] for 16QAM, but is different for 64QAM and 256QAM modulations.

Next, we briefly describe the so-called *ML bit demapper* [3, Formula (7)], which operates according to the maximum likelihood criterion. It follows the convention that decoding in bit-interleaved coded modulation is performed by applying an ML bit demapper followed by de-interleaving and Viterbi decoding. A suboptimal simplified branch metric that is obtained by the log-sum approximation, i.e., $\log(\sum_j Z_j) \backsimeq \max_j \log(Z_j)$, as typically occurs in channels with high signal-to-noise ratio (SNR), is also given in [3, Formula (9)]. We found that the ML bit demapper metric $\{\bar{q}_j^{(m)}(\cdot,\cdot)\}_{1\leq j\leq m, m\geq 1}$ and its simplification $\{q_j^{(m)}(\cdot,\cdot)\}_{1\leq j\leq m, m\geq 1}$ for 2^{2m}-QAM can also be expressed in recursive forms as follows.

$$\begin{aligned} \bar{q}_1^{(m)}(c,r) &= \sum_{k=1}^{2^{m-1}} \exp\left\{-\frac{(r-(2k-1)(2c-1))^2}{2\sigma^2}\right\} \\ \bar{q}_j^{(m)}(c,r) &= \bar{q}_{j-1}^{(m-1)}\left(c, 2^{m-2}u + r\right) \\ & \quad +\bar{q}_{j-1}^{(m-1)}\left(c, (-1)^j\left(2^{m-2}u - r\right)\right) \\ q_1^{(m)}(c,r) &= -2\sum_{k=1}^{2^{m-1}-1} (|r-2(2c-1)k| - 2k) \\ & \quad -2^m(2c-1)r + 1 \\ q_j^{(m)}(c,r) &= q_{j-1}^{(m-1)}\left(c, (-1)^j(2^{m-2}u - |r|)\right) \\ & \quad -2^m|r| + 2^{2(m-1)}, \end{aligned}$$

where σ^2 is the variance of the additive white Gaussian noise and $m = \log_2(M) \geq 2$, $2 \leq j \leq m$.

D. Complexity Comparison of the Metrics Introduced Previously

All the metrics introduced in the previous subsection are *piece-wise linear* functions of r for given c except the ML bit demapper $\{\bar{q}_j^{(m)}(\cdot,\cdot)\}_{1\leq j\leq m, m\geq 1}$, which is an apparent *non-linear* function in r. For this reason, it is indicated in [3]

[6] The IEEE 802.11a standard did not specify the interleaver for 256QAM transmission. Here, we simply extend its design philosophy for 16QAM and 64QAM transmission to obtain an extension interleaver for use of 256QAM transmission. To be specific, 96 256QAM quadrature components are tabularized in the same fashion as 16QAM, where each component is now comprised of four bits instead of two bits, and circular shift (from bottom to top) is repeated $(i-1)$ times for those bits belonging to the same quadrature component that locates at ith column.

[7] The amplitude spacing, u, is 2 for all QAM considered in this work.

[8] Their simplified soft-output demapper has been appeared in a book published in 1997 [14]. In the book, the soft-output demapper is heuristically obtained through a direct derivation, as opposed to the simplified-from-LLR-decision approach taken by Tosato and Bisaglia.

that the computational complexity of the ML bit demapper is classified to be much higher than its simplified counterpart $\{q_j^{(m)}(\cdot,\cdot)\}_{1\le j\le m, m\ge 1}$. We then turn to the complexity comparison of the remaining four piece-wise linear metrics.

For a class of piece-wise linear metrics, it is reasonable to compare their computational complexity in software implementation by the number of intervals within which the slope remains constant. This number determines the number of comparisons required for the input value r. As the four piece-wise linear metrics share similar recursive forms, their computational complexities are determined by the complexities of their first-bit metrics. It can be easily obtained that at $c = 1$, the numbers of the fixed-slope intervals for the first-bit metrics are given by:

m=	1	2	3	4	$\cdots$	general formula
$f_1^{(m)}(1,r)$	1	2	4	6	$\cdots$	$\max\{2(m-1),1\}$
$g_1^{(m)}(1,r)$	1	1	1	1	$\cdots$	1
$\bar{g}_1^{(m)}(1,r)$	2	4	6	8	$\cdots$	$2m$
$q_1^{(m)}(1,r)$	1	2	4	8	$\cdots$	2^{m-1}

This shows that the computational complexity of proposed metric $f_1^{(m)}(1,r)$ that is obtained from bit-wise decomposition of M-ary symbol metric is only secondary to the Tosato and Bisaglia's simplified metric $g_1^{(m)}(1,r)$ at $c = 1$.

It should be noted that at $c = 0$, $f_j^{(m)}(0,r) = g_j^{(m)}(0,r) = \bar{g}_j^{(m)}(0,r) = 0$ for all $1 \le j \le m$ and $m \ge 1$, and therefore, no computation effort is required. However, at $c = 0$, metric $q_1^{(m)}(0,r)$ remains piece-wise linear with the same number of fixed-slope intervals. Also, the margins of the fixed-slope intervals for $q_1^{(m)}(1,r)$ may be different from those for $q_1^{(m)}(0,r)$; hence, additional effort may need to be placed to adjust the margins according to the value of c. This makes the simplified ML bit demapper a least preferred one from the computational complexity standpoint.

III. Performance Evaluation Over AWGN Channels

Fig. 2 summarizes the simulation performances under the AWGN channel when 64QAM modulation is employed for *symbol-based ML decision* in (1), our *proposed bit-decomposed metrics*, the Tosato and Bisaglia's *simplified bit metrics*, the *ML bit demapping metrics and its simplification*, and the *hard-decision decoding system*. They are respectively abbreviated as *Symbol-ML*, *Soft-proposed*, *Soft-TB*, *ML-bit*, *ML-bit simplified* and *Hard* in all subsequent figures. From Fig. 2, we observed that at BER = 10^{-5}, *Soft-proposed* has 3.8 dB gain over *Hard*, but is 0.83 dB inferior to the ideal Symbol-ML under 64QAM modulation. More advantage can be obtained under 256QAM, where the gain of *Soft-proposed* over hard is enlarged to 5.1 dB. Note that although *Soft-proposed* and *Soft-TB* use different bit metrics under 64QAM modulation, they have comparable performance. The superiority of *Soft-proposed* over the *Soft-TB* will be more apparent if fading channels are considered instead of AWGN channels (cf. Figs. 8 and 9). Furthermore, *Soft-proposed* has indistinguishable performance to *ML-bit* and *ML-bit simplified* even though it has less computational complexity. As *Soft-TB*

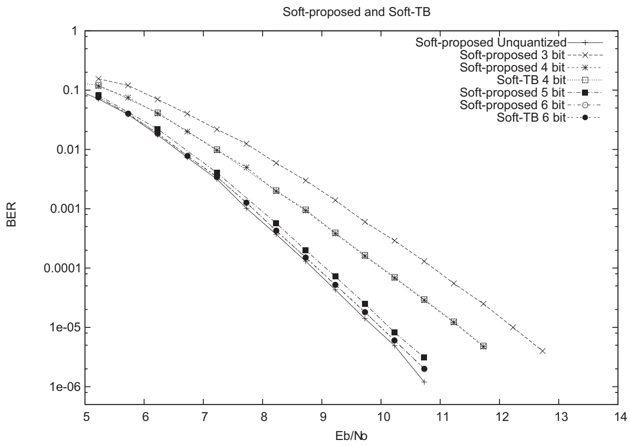

Fig. 3. Performance impact of quantization for 64QAM modulation.

is the only one that has less computational complexity than *Soft-proposed*, we only compare our proposed scheme with it in following subsections.

A. Effect of Quantization

Fig. 3 illustrates the performance impact of uniform quantization. Similar to [2], [7], the received scalar is first multiplied by the appropriate normalization factor in order to make the average QAM symbol power equal to unity, and then is quantized with the step size equal to $2 \times u$ divided by the number of quantization levels, where $u = 2$ is the amplitude spacing for QAM signals.

We observed that under 64QAM modulation, adopting 64-level quantizer to *Soft-proposed* and *Soft-TB* only yields 0.07 dB performance loss at BER = 10^{-5}. Hence, it is sufficient to take 6-bit quantization for the proposed bit-decomposed metrics to perform close to the unquantized system. Same conclusion can be made on Tosato and Bisaglia's simplified bit metrics. We then proceed to examine the robustness of these quantized bit metrics in terms of the above quantization levels against gain mismatch in the next subsection.

B. Imperfect Gain Control

Coded systems that quantize the matched filter output to more than two levels for use of subsequent digital manipulation require an analog-to-digital converter, whose level thresholds should depend on a correct measurement of the noise variance. Usually, the level-setting is effectively controlled by the automatic gain control (AGC) circuitry in a modem. In this subsection, we are interested in the sensitivity of decoder performance to an inaccurately quantized AGC signal.

Our performance comparisons between *Soft-proposed*, *Soft-TB* and *Hard* are employed at BER=10^{-5}. Due to different BER performances, different E_b/N_0's are accordingly used for each bit-decomposition approach. Specifically, under 64QAM modulation, we use 9.7 dB and 13.5 dB respectively for *Soft-proposed/Soft-TB* and *Hard* in order to obtain the required BER. The relative AGC mismatch without AGC drift is taken as u divided by the number of quantization levels [2], [7]. A drift to the above value is then caused by an inaccurate AGC circuitry.

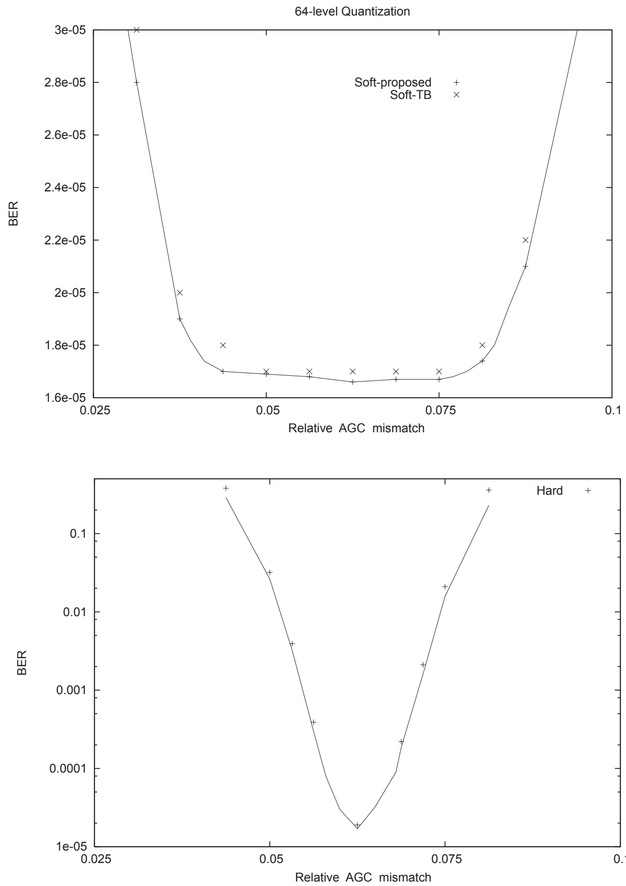

Fig. 4. Sensitivity to gain-mismatch for 64QAM. The taken values of E_b/N_0 for *Soft-proposed*/*Soft-TB* and *Hard* are respectively 9.7 dB and 13.5 dB. For a fair comparison, we first do 6-bit quantization on the received QAM signal using the same relative AGC mismatch as *Soft-proposed*/*Soft-TB* for *Hard*, and then do hard-demapping based on the quantization output. The ideal (without AGC drift) relative AGC mismatch is $2 \times 2/64 = 0.0625$.

From Fig. 4, we found that the performances of *Soft-proposed* and *Soft-TB* are quite insensitive to wide range of variation in AGC drift. The resultant BER remains between 1.7×10^{-5} and 2.0×10^{-5} over a relative AGC mismatch range of 0.0375$\sim$0.0875 for 64-level quantized 64QAM signals. This allows an AGC gain margin[9] of

$$\frac{|0.0375 - (0.0375 + 0.0875)/2|}{(0.0375 + 0.0875)/2} = \frac{|0.0875 - (0.0375 + 0.0875)/2|}{(0.0375 + 0.0875)/2} = 40\%.$$

However, for *Hard*, even if we allow BER to increase from 1.0×10^{-5} to 1.0×10^{-4}, the AGC gain margin is only

$$\frac{|0.070625 - 0.0625|}{0.0625} = \frac{|0.0625 - 0.054375|}{0.0625} = 13\%.$$

C. Effect of Phase Imperfection

In all previous simulations, perfect synchronization is implicitly assumed. However, the real systems often suffer certain degree of uncompensated oscillator instabilities and

[9]When AGC-drift goes up to 60%, the BER increases from 1.7×10^{-5} to 4.2×10^{-5}.

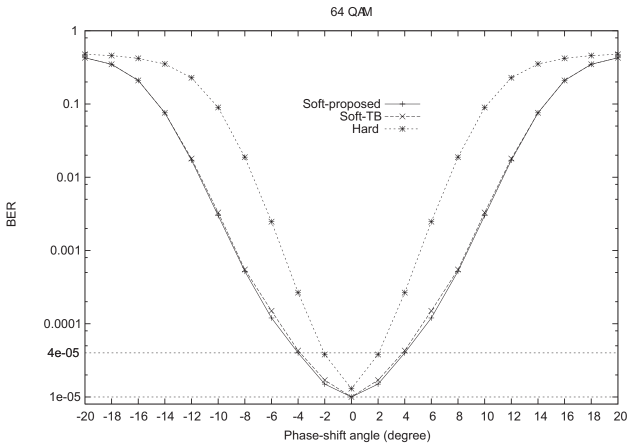

Fig. 5. Performance impact of the phase noise. The values of E_b/N_0 taken for *Soft-proposed*/*Soft-TB* and *Hard* are respectively 9.7 dB and 13.5 dB under 64QAM.

Doppler shifts even a carrier phase tracking circuitry is implemented at the receiver.

By introducing a bit interleaver before symbol modulation, no general expression between the symbol error and the bit error can be obtained. Therefore, the conventional technique that integrates the symbol error rate as a function of symbol phase imperfection ϕ with respect to a distribution of ϕ cannot be used to realize the relation between the bit error rate and phase imperfection. We accordingly establish the relation between the bit error rate and phase error ϕ by computer simulations.

It is obtained from simulations that under perfect gain control and no quantization, the minimum signal-to-noise ratios per information bit (E_b/N_0) to achieve the required BER of 10^{-5} are 9.7 dB and 13.5 dB for *Soft-proposed*/*Soft-TB* and *Hard* under 64QAM modulation, respectively. Thus, under the selected E_b/N_0's, we can observe from Fig. 5 that if BER is allowed to increase up to 4.0×10^{-5}, *Soft-proposed* and *Soft-TB* can tolerate up to $\pm 4^o$ phase drift, while *Hard* only allows $\pm 2^o$ phase drift. This result concludes that *Soft-proposed* and *Soft-TB* are less sensitive to phase drift than *Hard*.

IV. Realization of the Systematic Bit-Wise Decomposition Metric

Traditionally, realization of the Viterbi decoder can be divided into three units [6], [13]: the branch metric unit (BMU), the add-compare-select unit (ACSU) and the survivor memory unit (SMU). The input data is used in BMU to calculate the branch metrics for each new time step. These metrics are then fed to ACSU, which accumulates the branch metrics. The resultant accumulated path metric is stored in the path metric memory (PMM) according to the ACS-recursion. The SMU processes the decisions which are being made in ACSU, and outputs the estimated path with a latency of at least D, called the survivor depth.

In this section, we provide a systematic architecture for BMU, which avails the recursiveness nature of the proposed bit metric decomposition formulas, as depicted in Fig. 6. Our architecture only requires the first-bit function table, and can

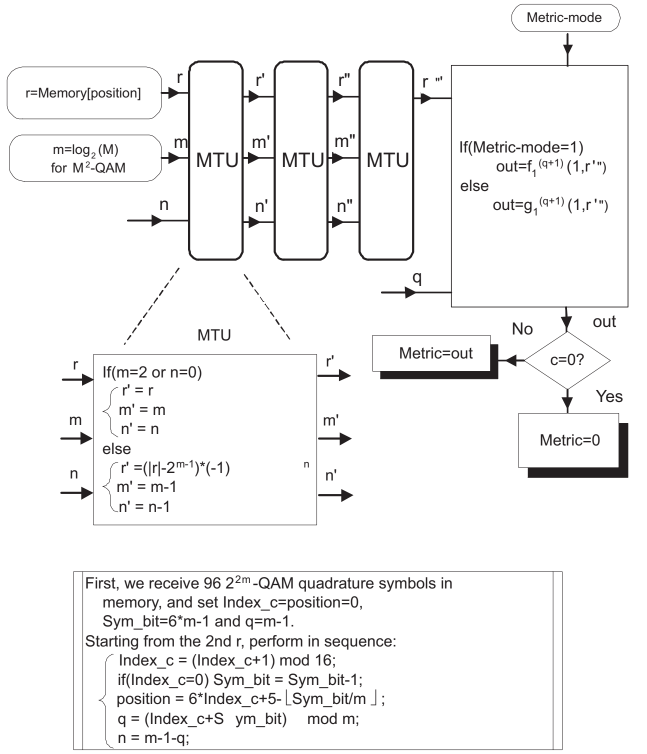

Fig. 6. A dual-mode BMU architecture with $(m_{\max}-2)$ serially connected MTU's can perform the bit metric evaluations for 2^{2m}-QAM, where $2 \le m \le m_{\max}$. Here, $m_{\max}=5$. All the constants in the formulas of Index_c, Sym_bit and position, such as 16, 6, and 5 $(=6-1)$ are chosen according to the 6×16 interleaver block used in IEEE 802.11a/g standard.

be applied for 2^{2m}-QAM modulations for every $2 \le m \le m_{\max}$, if $(m_{\max}-2)$ metric transition units (MTUs) are serially connected.

Under the setting of IEEE 802.11a/g, an OFDM signal consists of 96 real 2^m-PAM symbols, and each 2^m-PAM symbol was mapped from m coded-and-interleaved bits. The decoding sequences from left to right can be divided into 6 rows, where each row consists of 16 2^m-PAM symbols. As an example, the first row contains $\{r_0, r_6, r_{12}, \ldots, r_{90}\}$, and the symbols in $\{r_1, r_7, r_{13}, \ldots, r_{91}\}$ form the second row. An internal control variable, named `Index_c`, is used to keep the record of which column of QAM quadrature symbol block the BMU is currently used. Consequently, `Index_c` is initially zero for each new 96 QAM quadrature symbol block, and is updated according to the rule of $\texttt{Index\_c} = (\texttt{Index\_c}+1) \bmod 16$. Another internal control variable, `Sym_bit`, is used to adjust the demapped bit number in each QAM quadrature symbol according to the interleaver rule. It is equal to $(6 \times m - 1)$ initially for each new 96 QAM quadrature symbol block, and is reduced by one when `Index_c` equals 0. We also record the `position` of the QAM quadrature component (in the 96 QAM quadrature symbol block) that is currently used. As a result, $\texttt{position} = 6 \times \texttt{Index\_c} + 5 - \lfloor \texttt{Sym\_bit}/m \rfloor$, where $\lfloor \cdot \rfloor$ denotes the floor function. All the internal control variables are periodically updated at the time a new QAM quadrature symbol enters the BMU. Notably, for 2^{2m}-QAM demodulation, each QAM quadrature symbol has to be re-accessed m times; for example, the BMU needs to generate $192 = 2 \times 96$ soft bit metrics for 16QAM demodulation.

One can easily combine the implementation of both our metrics and Tosato and Bisaglia's simplified metrics by providing two first-bit metric function tables. As shown in Fig. 6, two metric calculation modes are set as:

"`Metric-mode`$=1$" is for *Soft-proposed*, and
"`Metric-mode`$=0$" is for *Soft-TB*.

A forth internal control variable, $q = (\texttt{Index\_c}+\texttt{Sym\_bit}) \bmod m$, is used to determine the bit metric function number. When q is decided, either function $f_1^{(q+1)}(\cdot,\cdot)$ or function $g_1^{(q+1)}(\cdot,\cdot)$ is used, depending on the `Metric-mode`. The last internal control variable, n, is simply $m-1-q$.

Our BMU requires two external input signals, which are *(i)* the received QAM quadrature symbol r that are derived from the proper position of the 96 symbol block, and *(ii)* $m = \log_2(M)$ if what has been received is M^2-QAM quadrature symbol.

Finally, since the soft bit metric equals zero when the branch bit c is zero, the BMU only evaluates bit metric values for $c = 1$. The case for "$c = 0$" is then handled by a check box appended at the output end of the BMU.

V. Concluding Remarks

In this paper, we obtained a recursive bit-decomposed metric formula through the approximation of symbol-based Euclidean metric. We subsequently compare the performances of the proposed soft bit-decomposed metric, the simplified bit metrics proposed in [12] and the straightforward hard-decision decoding system. As anticipated, the proposed soft bit-decomposed metric and the simplified bit metrics in [12] perform better than *Hard* in all respects.

The superiority of our proposed bit-decomposed metric over the simplified bit metrics proposed in [12] is a little more apparent under a fading environment and a higher QAM. By assuming a slowly fading channel with perfect channel knowledge as depicted in Fig. 7, the performance difference between these two methods is a little larger (than that under the AWGN channel) as shown in Figs. 8 and 9. We observed from Fig. 8 that in a Rayleigh flat fading environment, the performance superiority of *Soft-proposed* and *Soft-TB* over the *Hard* extends to 8.5 dB under 256QAM modulations at BER = 10^{-5}. The superiority extension remains large as 7.2 dB at BER = 10^{-5} in a frequency selective fading model defined in [1, Column 1, Tab. 10] as shown in Fig. 9. Besides, our proposed bit-decomposed scheme has comparable performance to *ML-bit* scheme and its simplification given in[3] under fading channels, in spite of the higher computational complexities of the latter two.

Acknowledgment

Authors would like to thank Prof. Luc Vandendorpe for his great help and comments. We would also like to thank the anonymous reviewers for their valuable comments.

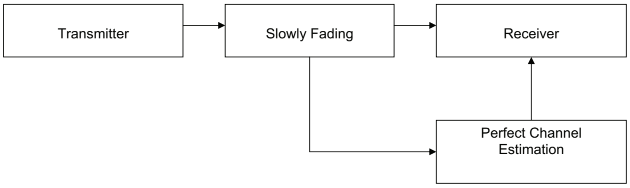

Fig. 7. Block diagram of a slowly fading channel with perfect channel knowledge. The channel fading considered can be either a simple frequency non-selective Rayleigh flat fading or a frequency-selective fading as defined in [11, Eq. (2.4)] with single transmit antenna ($M_t = 1$) and single receive antenna ($M_r = 1$).

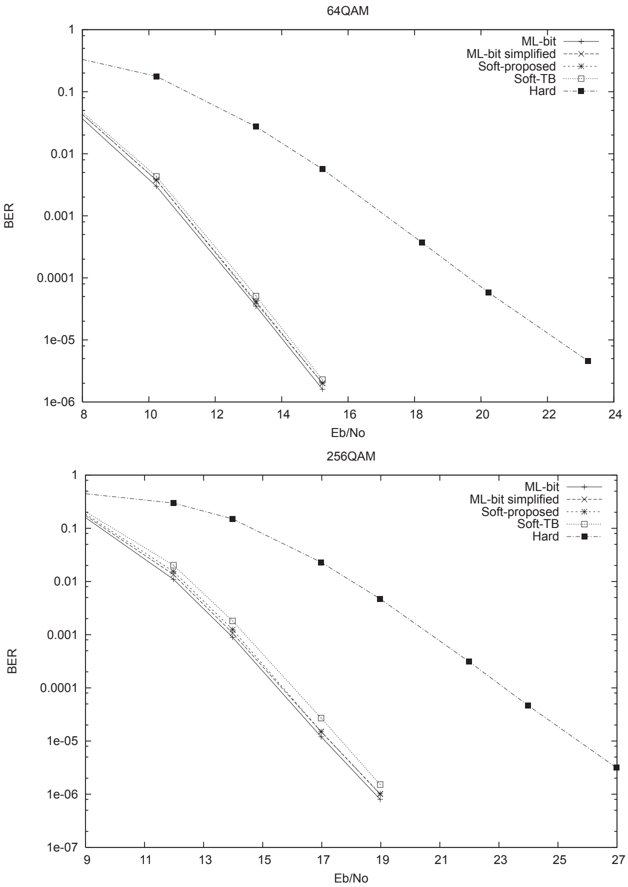

Fig. 8. System performances under Rayleigh flat fading channels. The performance superiority of *Soft-proposed* over *Hard* respectively extend to 8.1 dB, 8.5 dB under 64QAM, 256QAM modulations at BER = 10^{-5}.

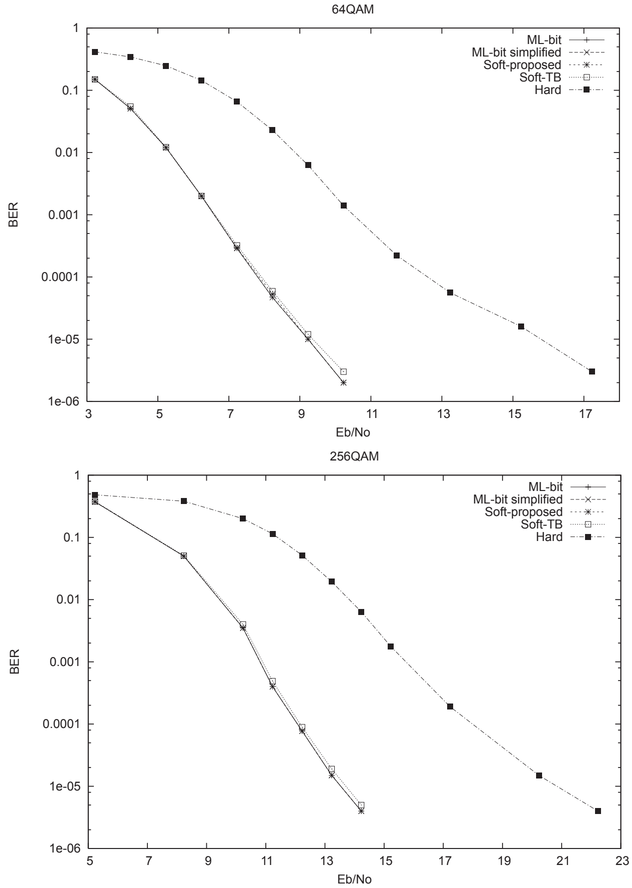

Fig. 9. System performances under frequency selective fading channel model defined in [1, Column 1, Tab. 10]. The performance superiority of *Soft-proposed* over *Hard* respectively extend to 6.5 dB, 7.2 dB under 64QAM, 256QAM modulations at BER = 10^{-5}.

REFERENCES

[1] Application Note 72, SPIRENT Communications, Inc., 2003.

[2] M. R. G. Butler, S. Armour, P. N. Fletcher, A. R. Nix, and D. R. Bull, "Viterbi decoding strategies for 5GHz wireless LAN systems," *IEEE Vehicular Technology Conference*, Sep. 2001, vol. 1, pp. 77–81.

[3] G. Caire, G. Taricco, and E. Biglieri, "Bit-interleaved coded modulation," *IEEE Trans. Inform. Theory*, vol. 44, no. 3, pp. 927–946, May 1998.

[4] C.-W. Chang and P.-N. Chen, "On bit-wise decomposition of M-ary symbol metric," *International Conference on Informatics Cybernetics and Systems (ICICS2003)*, Dec. 2003, pp. 905-910.

[5] ETSI TS 101 475, "Broadband Radio Access Networks (BRAN); HIPERLAN Type 2; Physical (PHY) Layer," v1.2.2, 2001.

[6] G. Fettweis, "Algebraic survivor memory management design for Viterbi detectors," *IEEE Trans. Commun.*, vol. 43, no. 9, pp. 2458–2463, Sep. 1995.

[7] J. A. Heller and I. M. Jacobs, "Viterbi decoding for satellite and space communication," *IEEE Trans. Commun.*, vol. 19, no. 5, pp. 835–848, Oct. 1971.

[8] IEEE Std 802.11a-1999, "Part 11: Wireless LAN Medium Access Control (MAC) and Physical Layer (PHY)Specifications: High-speed Physical Layer in the 5 GHz band," Sep. 1999.

[9] IEEE 802.11g-2003, "Part 11: Wireless LAN Medium Access Control (MAC) and Physical Layer (PHY) Specifications: Further Higher Data Rate Extension in the 2.4 GHz Band," Apr. 2003.

[10] R. Pyndiah, A. Picard, and A. Glavieux, "Performance of block turbo coded 16-QAM and 64-QAM modulations," in *Proc. IEEE GLOBECOM*, Nov. 1995, vol. 2, no. 13–17, pp. 1039–1043.

[11] W. Su, Z. Safar, and K. J. R. Liu, "Full-rate full-diversity space-frequency codes with optimum coding advantage," *IEEE Trans. Inform. Theory*, vol. 51, no. 1, pp. 229–249, Jan. 2005.

[12] F. Tosato and P. Bisaglia, "Simplified soft-output demapper for binary interleaved COFDM with application to HIPERLAN/2," *IEEE International Conference on Communications*, Apr./May 2002, vol. 2, pp. 664-668.

[13] C.-Y. Tsui, R.-S.-K. Cheng, and C. Ling, "Low power ACS unit design for the Viterbi decoder," *IEEE International Symposium on Circuits and Systems*, May 1999, vol. 1:30, pp. 137–140.

[14] R. Van Nee and R. Prasad, *OFDM for Wireless Multimedia Communications.* Norwood, MA: Artech House, 1997.

[15] E. Zehavi, "8-PSK trellis codes for a Rayleigh channel," *IEEE Trans. Commun.*, vol. 40, no. 5, pp. 873–884, May 1992.

Chia-Wei Chang (S'05) was born in Taipei, Taiwan, in 1980. He received the B.S. and M.S. degrees in communication engineering from the National Chiao-Tung University, Hsinchu, Taiwan, in 2002 and 2004, respectively. He currently pursues his Ph.D. degree in electrical, computer engineering of UCSD from 2005. Mr. Chang received the 2004 Prize of the Graduate Student thesis Contest from CIEE, Taiwan and $Calit^2$ Fellowship Award 2005 from UCSD. His research interests generally lie in information and coding theory, multimedia application, data dissemination and network coding.

Po-Ning Chen (S'93-M'95-SM'01) was born in Taipei, Taiwan, in 1963. He received the B.S. and M.S. degrees in electrical engineering from the National Tsing-Hua University, Hsinchu, Taiwan, in 1985 and 1987, respectively, and the Ph.D. degree in electrical engineering from University of Maryland, College Park, in 1994. From 1985 to 1987, he was with the Image Processing Laboratory, National Tsing-Hua University, where he worked on the recognition of Chinese characters. During 1989, he was with Star Tech. Inc., where he focused on the development of fingerprint recognition systems. In 1994, he joined Wan Ta Technology, Inc., as a Vice General Manager, conducting several projects on point-of-sale systems. In 1995, he became a Research Staff Member in the Advanced Technology Center, Computer and Communication Laboratory, Industrial Technology Research Institute, Taiwan, where he led a project on Java-based Network Managements. Since 1996, he has been an Associate Professor in the Department of Communications Engineering, National Chiao-Tung University, Hsinchu, Taiwan, and became a Full Professor in 2001. Dr. Chen received the 2000 Young Scholar Paper Award from Academia Sinica, Taiwan. His research interests generally lie in information and coding theory, large deviation theory, and distributed detection.

Yunghsiang S. Han (S'90-M'93) was born in Taipei, Taiwan, on April 24, 1962. He received the B. S. and M. S. degrees in electrical engineering from the National Tsing Hua University, Hsinchu, Taiwan, in 1984 and 1986, respectively, and the Ph. D. degree from the School of Computer and Information Science, Syracuse University, Syracuse, NY, in 1993. From 1993 to 1997 he was an Associate Professor in the Department of Electronic Engineering at Hua Fan College of Humanities and Technology, Taipei Hsien, Taiwan. From 1997 to 2004 he was with the Department of Computer Science and Information Engineering at National Chi Nan University, Nantou, Taiwan. He was promoted to Full Professor in 1998. From June to October 2001 he was a visiting scholar in the Department of Electrical Engineering at University of Hawaii at Manoa, HI, and from September 2002 to January 2004 he was the SUPRIA visiting research scholar in the Department of Electrical Engineering and Computer Science and CASE center at Syracuse University, NY. He is now with the Graduate Institute of Communication Engineering at National Taipei University, Taipei, Taiwan. His research interests are in wireless networks, security, and error-control coding.

Dr. Han is a winner of 1994 Syracuse University Doctoral Prize.